*Electronic Supplementary Information (ESI) for*

# Construction of Self-enhanced Photoelectrochemical Platform for L-cysteine Detection via Electron Donor-acceptor Type Coumarin 545 Aggregates

Hui Meng, Min Chen, Fangjing Mo, Jiang Guo, Pingkun Liu, Yingzi Fu*

Key Laboratory of Luminescent and Real-Time Analytical Chemistry (Southwest University), Ministry of Education, School of Chemistry and Chemical Engineering, Southwest University, Chongqing 400715, China



**List of Contents:**

* Corresponding author: *Yingzi Fu*

Tel: +86-023-68252277

E-mail address: fyzc@swu.edu.cn

# Contents

## 1. Reagents and apparatus

Coumarin 545 (10-(benzo[d]thiazol-2-yl)-2,3,6,7-tetrahydro-1H-pyrano [2,3-f]pyrido[3,2,1-ij]quinolin -11(5H)-one, 99%) was purchased from TCI Chemical Industry Development Co., Ltd. (Shanghai). L-cysteine (L-Cys, 99%), glutathione (GSH, 99%), lysine (Lys, 99%), proline (Pro, 99%), tryptophan ( Trp, 99%) and valine (Val, 99%) were obtained from Bailingwei Technology Co., Ltd. Triton X-100, cetyltrimethylammonium bromide (CTAB), absolute ethanol, potassium chloride (KCl, 99%), ferrocene (Fc), potassium dihydrogen phosphate ($KH_2PO_4$), hydrogen phosphate disodium ($Na_2HPO_4$) were acquired from Chengdu Kelong Chemical Co., Ltd. (Chengdu, China). Sodium dodecyl sulfate (SDS), tetrahydrofuran (THF, 99%), acetonitrile (99%), tetrabutylammonium hexafluorophosphate ((TBA)$PF_6$, 98%) were purchased from Sigma-Aldrich Co., Ltd. (American Life Science and Technology Group Corporation). 0.1 mol·$L^{-1}$ Phosphate buffer saline (PBS, containing 0.1 mol·$L^{-1}$ KCl) with different pH values were prepared by the different ratios of $KH_2PO_4$ and $Na_2HPO_4$ stock solutions. 5 mmol·$L^{-1}$ $[Fe(CN)_6]^{4-/3-}$ solution (pH=7.4) was prepared with $K_4Fe(CN)_6$ and $K_3Fe(CN)_6$. Healthy human urine samples offered by volunteers from Southwest University. This study was approved by the Human Ethics Committee of The Ninth People's Hospital of Chongqing (2021-LS-K-001) and volunteers were provided informed consent. All reagents are of analytical grade, without further purification before use. The ultrapure water was used in whole experiments (18.2 MΩ·$cm^{-1}$).

The Photoelectrochemistry (PEC) and electrochemical measurements were operated at CHI 440A (configured external LED lamp with the output power about 14 mW·$cm^{-2}$) and CHI 604D electrochemical workstations from Shanghai Chenhua Instrument Co., Ltd. (China).The UV-vis spectra were recorded by UV-2600 spectrophotometer from Shimadzu Instruments (Japan). The morphologies of materials were investigated by

scanning electron microscope (SEM, equipped with Xford-INCA energy dispersive X-ray spectrometer (EDX, Xford-INCA)) from Hitachi Instruments Co., Ltd. (Japan). The X-ray photoelectron spectroscopy (XPS) measurements were performed at Thermo Scientific Escalab 250Xi. The traditional three-electrode system was adopted in the PEC and electrochemical experiments, in which glassy carbon electrode (GCE, Φ=4 mm) or modified GCE was used as the working electrode, platinum metal as the counter electrode and the Ag/AgCl electrode as the reference electrode. The experiment temperature was 25± 1 ºC.

## 2. The synthesis process of S-C545, C-C545 and T-C545

The reprecipitation method was adopted for the synthesis of organic aggregates[1]. The precursor C545 (2 mg) was dissolved in tetrahydrofuran (THF, 1 mL) with ultrasonic treatment. Then, the C545/THF solution was injected dropwise into the 5 mL SDS solution (w=0.1%, anionic surfactant), stirring for 2 h. The synthesized orange red mixture was centrifuged and washed with ultrapure water several times, then dispersed in 1 mL of water to acquire aggregates solution (S-C545). Similarly, CTAB (cationic surfactant) and Triton X-100 (nonionic surfactant) were also used to prepare C-C545 and T-C545 aggregates respectively.

## 3. The preparation of PEC electrodes

Before the construction of PEC sensor, the GCE was polished with 0.5, 0.3 and 0.05 μm alumina powder, ultrasonically cleaned with water and absolute ethanol for several times until the electrode interface became mirror-like smooth. After drying at room temperature, 10 μL of different C545 aggregates was dropped on the clean GCE, respectively (denoted as S-C545/GCE, C-C545/GCE, T-C545/GCE), dried naturally for

subsequent experiments. Since the C545 aggregates, as a polycyclic aromatic compound, can be firmly attached on the GCE via π-π stacking interaction.

## 4. PEC and electrochemical measurement procedures

The PEC detection was carried out in 4 mL of 0.1 mol·L$^{-1}$ PBS (pH=7.4, including a series of concentrations of target L-Cys solution) on the CHI 440A electrochemical workstations, under periodic off-on-off (10-20-10 s) light radiation and at the applied voltage of 0.0 V. The electrochemical impedance spectroscopy (EIS) and cyclic voltammetry (CV) measurements were carried on CHI 604D electrochemical workstations in 5 mmol·L$^{-1}$ $[Fe(CN)_6]^{3-/4-}$ solution (pH=7.4).

## 5. CV and EIS characterizations

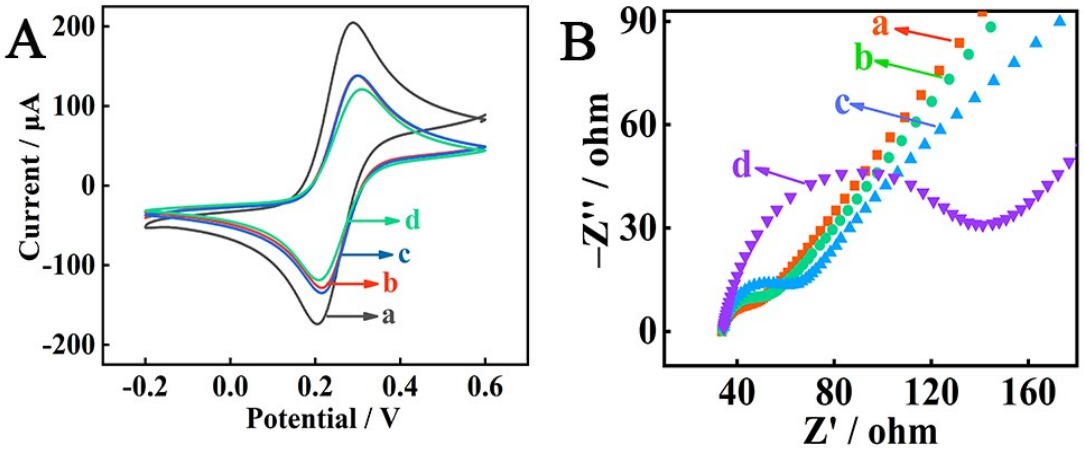


**Fig. S1.** (A) CV and (B) EIS plots of the different electrodes: (a) bare GCE, (b) S-C545/GCE, (c) C-C545/GCE, (c) T-C545/GCE.

## 6. The element mapping images of the prepared S-C545

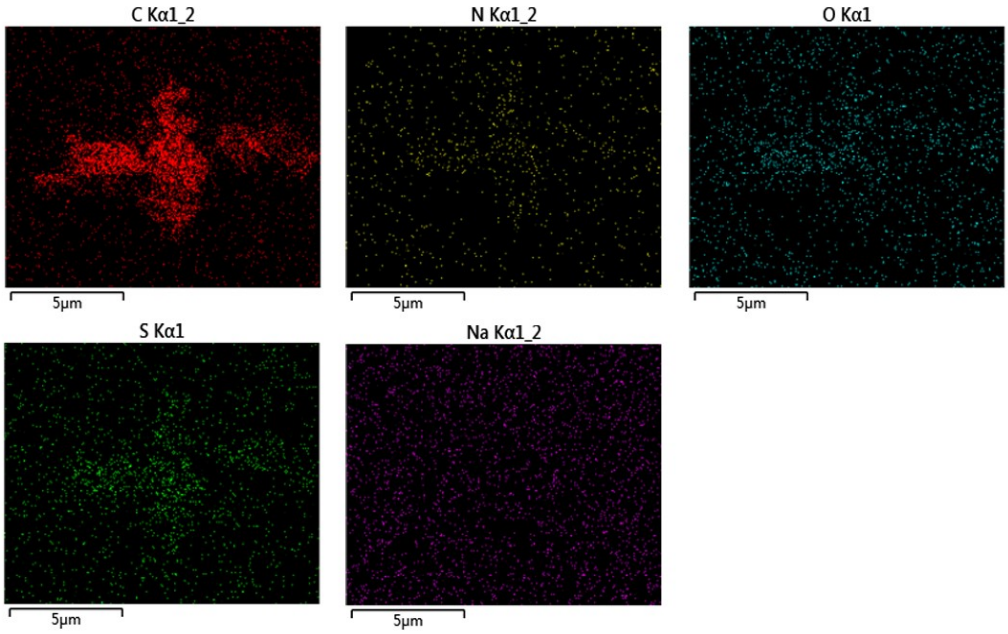


**Fig. S2.** The elemental mapping images of S-C545 including the elements of C, N, O, S, Na

## 7. Energy Band gap calculations of aggregates

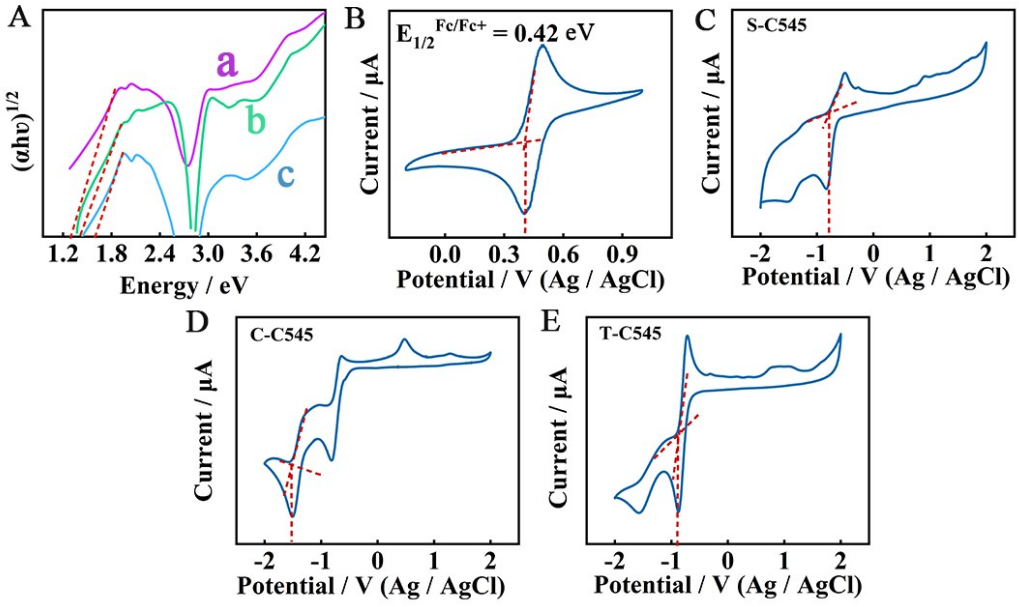


**Fig. S3.** (A) Tauc plots of indirect transitions: (a) S-C545, (b) C-C545 and (c) T-C545. (B) CV of bare GCE in a deoxygenated anhydrous acetonitrile solution containing 0.1 mol·$L^{-1}$ tetrabutylammonium hexafluorophosphate ($TBAPF_6$) and 0.5 mmol·$L^{-1}$ ferrocene (Fc) at scanning rate of 50 mV·$s^{-1}$. CV

of (C) S-C545/GCE, (D) C-C545 and (T) T-C545 as the working electrode in 0.1 mol·$L^{-1}$ $TBAP_6$ solutions under the same conditions. $E_{ox}$ was calculated from tangents of the oxidation peaks of the species.

The energy band gaps (Eg) of as-prepared S-C545, C-C545 and T-C545 were obtained by the following equation 1:[2]

$$\alpha h\upsilon = B(h\upsilon - Eg)^{n/2} \quad (1)$$

where α, h and $\upsilon$ are absorption coefficient, Planck constant and light frequency, respectively; Eg and B are band gap energy and constant, respectively. The n value is 1 or 4 mainly hinging whether the semiconductor has a direct or indirect band gap. The corresponding band gaps (Eg) of S-C545, C-C545 and T-C545 were successively determined as 1.30, 1.42 and 1.60 eV from the tangent to the linear of the plot of $(\alpha h\upsilon)^{(1/2)}$ versus ($h\upsilon$) (Fig. S3C~E).

The positions of the conduction band (CB) and valence band (VB) edges of S-C545, C-C545 and T-C545 were determined by their electron affinity (EA) and ionization potential (IP) using the following formulas (2-3). The energy levels of them can be obtained by counting its lowest unoccupied molecular orbital (LUMO) and highest occupied molecular orbital (HOMO) using the following formulas (4-5).

$$IP = -(4.80 - E_{1/2}^{Fc/Fc+} + E_{ox}) \quad (2)$$

$$EA = IP + Eg \quad (3)$$

$$E_{HOMO} = -(4.80 - E_{1/2}^{Fc/Fc+} + E_{ox}) \quad (4)$$

$$E_{LUMO} = E_{HOMO} + Eg \quad (5)$$

$E_{1/2}^{Fc/Fc+}$ is the formal potential of $Fc/Fc^+$, $E_{ox}$ is the oxidation initiation potential. Potentials are calibrated with the ferrocene/ferrocenium ($Fc/Fc^+$) couple, and the potential

of $Fc/Fc^+$ has an absolute energy level of 4.80 eV to vacuum.[3] At the scan rate of 50 $mV \cdot s^{-1}$ in 0.5 $mmol \cdot L^{-1}$ Fc solution, using bare GCE as working electrode, the $E_{1/2}^{Fc/Fc+}$ located at 0.42 V (curve c in Fig. S3B) was obtained. Eventually, the HOMO/LUMO are calculated as −3.59/−2.29 eV, −2.86/−1.44 eV and −3.49/−1.89 eV, respectively.

## 8. Optimization of experimental conditions

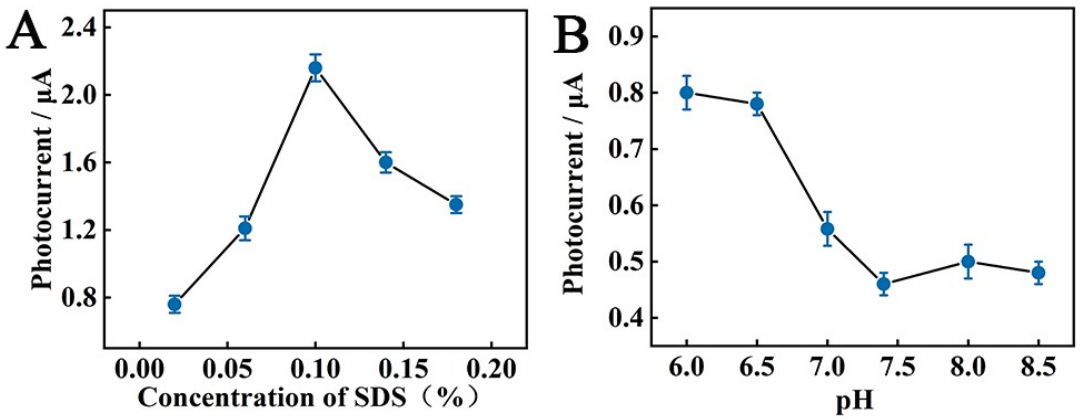


**Fig. S4.** The influence of (A) SDS concentration (wt%) and (B) the pH value toward the PEC sensor.

The amount of the SDS used for the synthesis of S-C545 and the pH value of the test solution were determined to acquire the best analytic performance of the PEC sensor. The photocurrent responses of corresponding S-C545 increase with the SDS concentration from 0.02% to 0.1%, however, the PEC responses reach a maximum value at 0.1% and decrease gradually as the increasing dosage (Fig. S4A). The isoelectric point of L-Cys is about 5.1.[4] When the pH value is over 5.1, the main form of L-Cys in the solution is L-Cys− anion. As the pH value elevates, the enhanced reducibility of L-Cys− causes the improved quenching effect on the sensing signal and the significant decrease of photocurrent. After the pH value reaching 7.4, the photocurrent signal tends to be stable

(Fig. S4.B). Therefore, 0.1% SDS-assisted S-C545 was selected as photoactive matrix to prepare the PEC sensor, additionally, the PEC detection was performed under the condition of pH 7.4.

## 9. Calculations about limit of detection

The limit of detection (LOD) and limit of quantitation (LOQ) were calculated in details.[5] The Parallel measurements for blank samples were performed six times. The averaged photocurrent is 2.085 μA with standard deviation ($S_B$) of 0.043. It is found that the photocurrent differences ($\Delta I$) linearly depends on the logarithm of L-Cys concentration ($c$) with signal-to-noise ratio (S/N = $k_1$) of 3. So when the $I_B$ is zero ($I_B$ = 0), the smallest detectable negative PEC signal is expressed as

$$I_L = I_B + k_1 S_B = -0.129$$

According to the linear regression equation $\Delta I = -0.25 \lg c - 0.28$, the LOD was calculated as $2.5\times10^{-10}$ mol·mL$^{-1}$. [6]

## 10. Stability of the PEC sensing platform

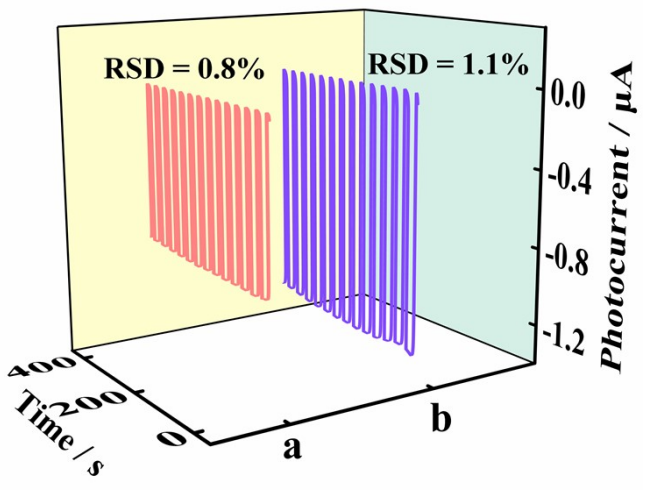

**Fig. S5.** Time-dependent PEC responses in (a) $10^{-5}$ mol·L$^{-1}$ and (b) $10^{-7}$ mol·L$^{-1}$ L-Cys under periodic off-on illumination for 400 s

The stability of the proposed PEC sensor for L-Cys detection was carried out under periodic off–on–off light for 400 s. As depicted in Fig. S5, the relative standard deviation (RSD) for the PEC responses of L-Cys ($10^{-5}$ and $10^{-7}$ mol·L$^{-1}$) is 0.8% and 1.1% respectively, proving the good stability.

## 11. Selectivity of the PEC sensor

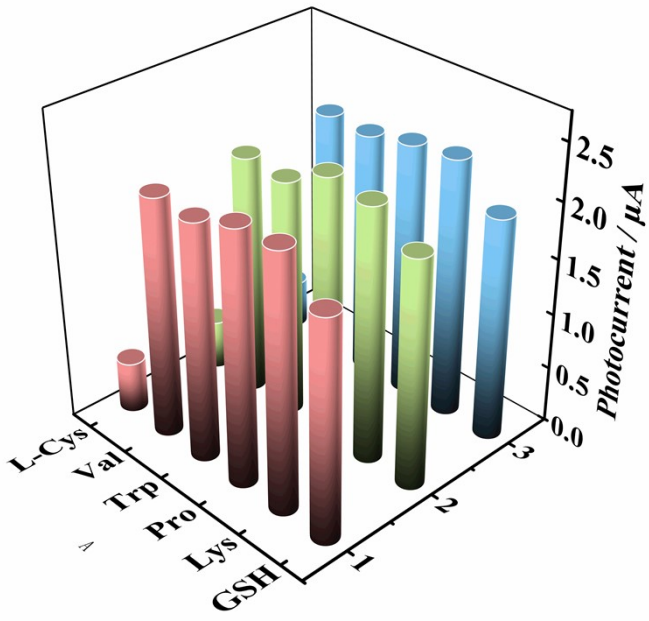


**Fig. S6.** The selectivity of the PEC sensor containing different interferences: Val ($10^{-4}$ mol·L$^{-1}$), Trp ($10^{-4}$ mol·L$^{-1}$), Pro ($10^{-4}$ mol·L$^{-1}$), Lys ($10^{-4}$ mol·L$^{-1}$) and GSH ($10^{-6}$ mol·L$^{-1}$)

The selectivity was evaluated by adopting several interfering substances in control experiments such as glutathione (GSH, $10^{-6}$ mol·L$^{-1}$), Lysine (Lys, $10^{-4}$ mol·L$^{-1}$), Proline (Pro, $10^{-4}$ mol·L$^{-1}$), Tryptophan (Trp, $10^{-4}$ mol·L$^{-1}$) and valine (Val, $10^{-4}$ mol·L$^{-1}$). From Fig. S6, as the concentration of GSH was lower than $10^{-6}$ mol·L$^{-1}$, little effect on PEC analysis. Besides, the PEC responses of Lys, Pro, and Val show an evident increase

compared with the L-Cys. Hence, the above results indicate that the PEC sensor is provided with good selectivity for detection of L-Cys.

## 12. Comparison of other analytical methods

The PEC sensor constructed by S-C545 with D-A configuration was compared with the previously reported analytic methods for L-Cys detection. The proposed PEC sensor demonstrated the wider linear range and lower LOD. It is primarily on account of the self-enhanced effect of the D-A type photoelectric material without the addition of electron donors, which may lessen the background interference, thereby improve the performance of the PEC sensor to some extent (Table S1).

**Table S1** Comparison for different methods for L-Cys detection

| Analysis method | Linear range ($mol \cdot L^{-1}$) | LOD ($mol \cdot L^{-1}$) | Reference |
|---|---|---|---|
| **CV** | $1.0\times10^{-6}$~$1.1\times10^{-6}$ | $3.1\times10^{-7}$ | [7] |
| **CS** | $1.0\times10^{-6}$~$1.0\times10^{-4}$ | $9.2\times10^{-8}$ | [8] |
| **ECL** | $1.3\times10^{-6}$ ~$3.5\times10^{-5}$ | $8.7\times10^{-7}$ | [9] |
| **PEC** | $2.0\times10^{-7}$ ~ $1\times10^{-6}$ | $5.0\times10^{-8}$ | [10] |
| **PEC** | $1.0\times10^{-9}$ ~ $1\times10^{-3}$ | $2.5\times10^{-10}$ | **This work** |

**Abbreviation:** Colorimetric sensing (CS), Electrochemiluminescence (ECL)

## 13. The real sample analysis

Additionally, the feasibility of the proposed sensor in biological samples was explored, the analysis was conducted in healthy human urine samples. The human urine was centrifuged, diluted 50 times and the pH was adjust to 7.4. Afterwards, a series concentrations of L-Cys were added into the diluted human urine sample.

The recovery rates of L-Cys were calculated via the standard addition method. As listed in Table S2, the recovery concentration was calculated through the obtained regression equation, and the recovery rate ranges from 97% to 103.0% with the RSD (2.6%~3.5%). The above results show that the self-enhanced PEC sensor underlies the foundation for the detection of L-Cys applied in real human samples

**Table S2.** Determination of L-Cys in human urine samples

| Sample | Spiked(mol·L$^{-1}$) | Found(mol·L$^{-1}$) | Recovery/% | RSD/% |
|---|---|---|---|---|
| **1** | $1.0\times10^{-4}$ | $0.97\times10^{-4}$ | 97.0 | 2.8 |
| **2** | $1.5\times10^{-6}$ | $1.54\times10^{-6}$ | 102.6 | 2.6 |
| **3** | $1.0\times10^{-8}$ | $1.03\times10^{-8}$ | 103.0 | 3.5 |

## 14. References


1 H. R. Chung, E. Kwon, H. Oikawa, H. Kasai; H. Nakanishi,. Cryst Growth Des., 2006, 294, 459-463.

2 Q. Wang, Y. F. Ruan, W. W. Zhao, P. Lin, J. J. Xu and H. Y. Chen, *Anal. Chem.* **2018**, 90, 3759-3765.

3 T. Edvinsson, , C. Li, , N. Pschirer, J.SchNeboom, F. Eickemeyer and R. Sens, *J. Phys. Chem. C*, 2007, 111, 15137-15140.

4 M. Zhou, J. Ding, L. P. Guo and Q. K. Shang, *Anal. Chem.*, 2007, 5328-5335; N. Spãtaru, B. V. Sarada, E. Popa, D. A. Tryk and A. Fujishima, *Anal. Chem.,* **2001** 514-519.

5 C. Wang, Q. Han, P. K. Liu, G. Zhang, L. Song, X. Zou and Y. Z. Fu, *ACS Sensors*, **2021**, 6, 252-258.

6 A. E. Radi, J. L. AceroŚanchez, E. Baldrich and C. K. O'Sullivan, *J. Am. Chem. Soc.*, **2006**, 117-124.

7 .K. Ozoemena, P. Westbroek, T. Nyokong, *Electrochem. Commun.*, **2001**, 3, 529-534.

8 L. Xiao, Y. Y. Xi, J. Q. Sha, T. Han, C. J. Du, S Y. Jun and Y. Q. Lan, *ACS Appl. Mater. Interfaces*, **2019**, 11, 18, 16896-16904.

9 L. Hua, Han, H.; Zhang, X., *Talanta*, **2009**, 77, 1654-1659.

10 Y. H. Zhu, Z. W. Xu, K. Yan, H. Zhao and J. D. Zhang, *ACS Appl. Mater. Interfaces*, **2017**, 9, 40452-40460.